Torsion Spring Oscillator with Dry Friction

Eugene I. Butikov

Saint Petersburg State University, Saint Petersburg, Russia

Abstract

Free and forced oscillations of a torsion spring pendulum damped by viscous and dry (Coulomb) friction are investigated analytically and with the help of computer simulations. An idealized mathematical model of dry friction described by the so-called z-characteristic is assumed. This simple physical model can explain many peculiarities in behavior of various oscillatory systems with dry friction. The amplitude of free oscillations diminishes under dry friction linearly, and the motion stops after a final number of cycles. In the sinusoidally driven pendulum with dry friction, the amplitude of forced oscillations grows linearly without limit at resonance if the threshold is exceeded. At strong enough non-resonant sinusoidal forcing dry friction causes transients that typically lead to periodic steady-state regimes of symmetric non-sticking forced oscillations which are independent of initial conditions. However, at the subharmonic sinusoidal forcing interesting peculiarities of the steady-state response are revealed such as multiple regimes of asymmetric oscillations that depend on initial conditions. Under certain conditions simple dry friction pendulum shows complicated stick-slip motions and chaos.

Keywords: dry friction, dead zone, sinusoidal forcing, resonance, threshold, asymmetric steady-state oscillations.

1. Introduction

Mechanical vibration systems with combined viscous and dry (Coulomb) friction are of considerable importance in numerous applications of dynamics in engineering. When friction is viscous, the spring oscillatory systems are described by linear differential equations. This case allows an exhaustive explicit analytical solution which is usually studied in undergraduate courses at universities and can be found in most textbooks on general physics. However, the influence of dry friction on oscillatory systems remains as a rule beyond the scope of the academic literature and traditional physics courses.

Dry friction results in a nonlinearity. With dry friction, the system acquires a non-smooth, discontinuous nonlinear character. If the coefficient of dry friction is sufficiently small, the oscillating body slides under harmonic forcing and its velocity is zero only for the instant when it passes through zero, that is, when the direction of motion reverses. This kind of motion of dry friction oscillator with no stick phase is usually referred to as a pure slip (non-sticking) motion. At large enough friction coefficient sticking may occur: the body remains at rest for a finite time during the driving cycle after the velocity of the oscillator reaches zero. A detailed historical review on dry friction and stick-slip phenomena can be found in [1].

Dry friction as a nonlinearity is the current focus of research activities. Even the simplest dry friction model, the Coulomb friction, can explain the principal peculiarities in motion of dry friction oscillator. Damping of free oscillations under dry friction is very clearly described in the textbook of Pippard [2] (see also [3]). Different approaches to the problem are discussed in [4]–[5]. Den Hartog [6] was first to solve in 1930 the periodic sliding response of a harmonically forced oscillator with both viscous and dry-friction damping. Later on the analytical solutions of

non-sticking responses were widely discussed in the contemporary scientific literature (see [7]–[13] and references therein). The problem was treated by using a number of various analytical and numerical techniques. In recent years, there has been an increasing interest in periodic and chaotic motions of discontinuous dynamical systems because of their important role in engineering (see, for example, [14]).

In the literature the analytical solution to the problem of oscillations in a system with dry friction is usually obtained by a simple method of stage-by-stage integration of the differential equations which describe the system. These equations are linear for the time intervals occurring between consecutive turning points. The intervals are bounded by the instants at which the velocity is zero. The complete solution is obtained by joining together these half-cycle solutions for consecutive time intervals. By exploiting the piecewise linear nature of the relevant differential equations, explicit solutions can be found between the successive stops.

In this paper we are concerned with free oscillations of a torsion spring pendulum, and with forced oscillations of the pendulum kinematically driven by an external sinusoidal force, when damping is caused by dry (Coulomb) friction, and both by viscous and dry friction. Mathematically, the pendulum driven by an external force is equivalent to the spring-mass system with the body residing on the horizontally oscillating base. The simple formulae of analytical solutions are confirmed by graphs obtained in computer simulations. New results are related with quantitative description of the resonant growth of oscillations under sinusoidal forcing, and with closed-form analytical solutions at sub-resonant frequencies describing multiple asymmetric steady-state regimes whose characteristics depend on the initial conditions.

2. The physical system

The rotating component of the torsion spring oscillator investigated in the paper is a balanced flywheel whose center of mass lies on the axis of rotation (figure 1), similar to devices used in mechanical watches. A spiral spring with one end attached to the flywheel flexes when the flywheel is turned. The other end of the spring is attached to the exciter — a driving rod, which can be turned by an external force about the axis common with the flywheel axis. The spring provides a restoring torque whose magnitude is proportional to the angular displacement of the flywheel from that of the driving rod. In other words, the flywheel is in equilibrium (the spring is unstrained) when the rod of the flywheel is parallel to the driving rod.

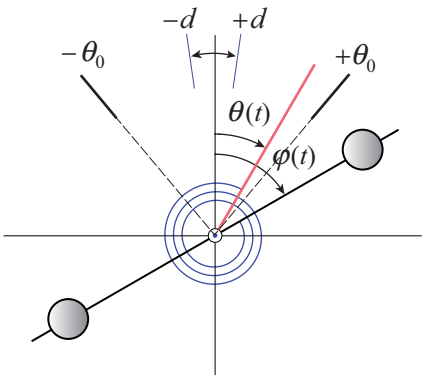

Figure 1: Schematic diagram of the driven torsion oscillator with dry friction

In the case of unforced (free, or natural) oscillations in an isolated system, the motion is initiated by an external influence which occurs before a particular instant. This influence determines the initial mechanical state of the system, that is, the displacement and the velocity of the

oscillator at the initial instant. These initial conditions determine the amplitude and phase of subsequent free oscillations, whose frequency and damping do not depend on initial conditions and are determined solely by the physical properties of the system.

Oscillations are called forced if an oscillator is subjected to an external periodic influence whose effect on the system can be expressed by a separate term, a periodic function of the time, in the differential equation of motion. We are interested in the response of the system to the periodic external force. The behavior of oscillatory systems under periodic external forces is one of the most important issues in the theory of oscillations. A noteworthy distinctive characteristic of forced oscillations is the phenomenon of resonance, in which a small periodic disturbing force can produce an extraordinarily large response in the oscillator. Resonance is found everywhere in physics and so a basic understanding of this fundamental problem has wide and various applications. The phenomenon of resonance depends upon the whole functional form of the driving force and occurs over an extended interval of time rather than at some particular instant. In this paper we draw attention to peculiarities of resonance in an oscillator with dry friction.

In our model of an oscillatory system, free oscillations of the flywheel occur when the driving rod is immovable ($\theta = 0$). Forced oscillations are excited when the driving rod rotates back and forth through an angle θ_0 sinusoidally about its middle position: $\theta(t) = \theta_0 \sin \omega t$. This mode differs from the dynamical mode considered usually in textbooks, according to which oscillations are excited by a given external force exerted on the system. Our mode can be called kinematical, because in this mode oscillations are excited by forcing one part of the system (the driving rod) to execute a given motion (in our case a simple harmonic motion). This kinematical mode is especially convenient for observation, because the motion of the exciter can be seen simultaneously with oscillations of the flywheel.

In the Coulomb model of dry friction, as long as the system is moving, the magnitude of dry friction is assumed to be constant, and its direction is opposite that of the velocity, that is, its direction changes each time the direction of the velocity changes. When the system is at rest, the force of static dry friction takes on any value from some interval $-F_{\max}$ to $F_{\max}$. The actual value of static frictional force can be found from the requirement of balancing the other forces exerted on the system. In other words, the force of static friction adjusts itself to make equilibrium with other external forces acting on the body. The magnitude of the force of kinetic dry friction is assumed in this model to be equal to the limiting force $F_{\max}$ of static friction.

In real physical systems dry friction is characterized by more complicated dependencies on the relative velocity (see, for example, [15]). The limiting force of static friction is usually greater than the force of kinetic friction. When the speed of a system increases from zero, kinetic friction at first decreases, reaches a minimum at some speed, and then gradually increases with a further increase in speed. These peculiarities are ignored in the idealized z-characteristic of dry friction. Nevertheless, this idealization allows us to understand many important features of oscillations in real physical systems.

In our model of a torsion oscillator some amount of dry friction can exist in the bearings of the flywheel axis. Because the magnitude of static frictional torque can assume any value up to $N_{\max}$, there is a range of values of angular displacement called the stagnation interval or dead zone in which static friction can balance the restoring elastic torque of the strained spring. At any point within this interval the system can be at rest in a state of neutral equilibrium, in contrast to a single position of stable equilibrium provided by the spring in the case of viscous friction.

The stagnation interval extends equally to either side of the point at which the spring is unstrained. The stronger the dry friction in the system, the more extended the stagnation interval. The boundaries of the interval $\pm d$ are determined by the limiting torque $N_{\max}$ of static friction.

In figure 1 these boundaries $-b$ and $+b$ are shown for the case in which the driving rod is in its middle position $\theta = 0$.

3. The differential equation of the oscillator

The rotating flywheel of the torsion oscillator is simultaneously subjected to the restoring torque $-D(\varphi - \theta)$ produced by the spring, the torque $-B\dot{\varphi}$ of viscous friction which is proportional to the angular velocity, and the torque N_{fr} of kinetic dry friction. The differential equation describing the rotational motion of the flywheel with moment of inertia J is thus

$$J\ddot{\varphi} = -D(\varphi - \theta_0 \sin \omega t) - B\dot{\varphi} + N_{\text{fr}}. \tag{1}$$

The torque N_{fr} is directed oppositely to angular velocity $\dot{\varphi}$, and is constant in magnitude while the flywheel is moving, but may have any value in the interval from $-N_{\max}$ up to $N_{\max}$ while the flywheel is at rest:

$$N_{\text{fr}}(\dot{\varphi}) = -N_{\max} \operatorname{sign} \dot{\varphi} = \begin{cases} -N_{\max} & \text{for} \quad \dot{\varphi} > 0, \\ N_{\max} & \text{for} \quad \dot{\varphi} < 0. \end{cases} \tag{2}$$

Here $N_{\max}$ is the limiting value of the static frictional torque. It is convenient to express the value $N_{\max}$ in terms of the maximal possible deflection angle d of the flywheel at rest, when the driving rod (see figure 1) is immovable at its middle position $\theta = 0$: $N_{\max} = Dd$. The angle d corresponds to the boundary of the stagnation interval. Dividing all terms of equation (1) by J, we get

$$\ddot{\varphi} + 2\gamma\dot{\varphi} + \omega_0^2 d \operatorname{sign} \dot{\varphi} + \omega_0^2 \varphi = \omega_0^2 \theta_0 \sin \omega t. \tag{3}$$

The damping constant γ is a measure of the intensity of viscous friction. It is introduced here by the relation $2\gamma = B/J$. The frequency $\omega_0 = \sqrt{D/J}$ characterizes undamped natural oscillations. The sign $\dot{\varphi}$ function is meant to take the undetermined values between 1 and -1 at zero, which corresponds to stick phase. The actual value of the static dry friction torque is such that the system is in equilibrium. The differential equation (1) for an oscillator with dry friction, as well as equation (3), is nonlinear because the torque $N_{\text{fr}}(\dot{\varphi})$ abruptly changes when the sign of $\dot{\varphi}$ changes at the extreme points of oscillation. This is the so-called Fillippov system [16]. In the idealized case of the z-characteristic this is a piecewise smooth system, and we may consider the following two linear equations instead of Eq. (3):

$$\ddot{\varphi} + 2\gamma\dot{\varphi} + \omega_0^2(\varphi + d) = \omega_0^2 \theta_0 \sin \omega t \qquad \text{for} \quad \dot{\varphi} > 0, \tag{4}$$

$$\ddot{\varphi} + 2\gamma\dot{\varphi} + \omega_0^2(\varphi - d) = \omega_0^2 \theta_0 \sin \omega t \qquad \text{for} \quad \dot{\varphi} < 0. \tag{5}$$

Whenever the sign of the angular velocity $\dot{\varphi}$ changes, the pertinent equation of motion also changes. The nonlinear character of the problem reveals itself in alternate transitions from one of the linear equations (4)–(5) to the other.

4. Damping of free oscillations under dry friction

For the case of free (unforced) oscillations the right-hand side of equations (4)–(5) is zero. In case the dry friction is absent (the dead zone vanishes: $d = 0$), damping of free oscillations occurs solely due to viscous friction. For this idealized case the differential equation of motion becomes linear. It has a well known analytical solution, according to which the amplitude of free oscillations under viscous friction decreases exponentially with time. That is, the consecutive

maximal deflections of the oscillator from its equilibrium position form a diminishing geometric progression because their ratio is constant.

In an idealized linear system such oscillations continue indefinitely, their amplitude asymptotically approaching zero. The duration of exponential damping can be characterized by a conventional decay time $\tau = 1/\gamma$. The exponential character of damping caused by viscous friction follows from the proportionality of friction to velocity. Some other relationship between friction and velocity produces damping with different characteristics.

The solution to equations (4)–(5) for non-zero dry friction ($d \neq 0$) can be found by using the method of the stage-by-stage integration of each of the linear equations for the half-cycle during which the direction of motion is unchanged. These solutions are then joined together at the instants of transition from one equation to the other in such a way that the displacement at the end point of one half-cycle becomes the initial displacement at the beginning of the next half-cycle. This array of solutions continues until the end point of a half-cycle lies within the dead zone.

An important feature of free oscillations damped by dry friction is that the motion completely ceases after a finite number of cycles. As the system oscillates, each subsequent change of its velocity occurs at a smaller displacement from the mid-point of the stagnation interval. Eventually the turning point of the motion occurs within the stagnation interval, where static friction can balance the restoring torque of the spring, and so the motion abruptly stops. At which point of the interval this event occurs, depends on the initial conditions, which may vary from one situation to the next.

These characteristics are typical of various mechanical systems with dry friction. For example, dry friction may be encountered in measuring instruments, such as a moving-coil galvanometer, in which readings are taken with a needle. The needle of the coil may come to rest at any point of the stagnation interval on either side of the dial point which gives the true value of the measured quantity. This circumstance explains the origin of random errors inevitably occurring in the readings of moving-coil measuring instruments. The larger the dry friction, the larger the errors of measurement.

In order to find the fundamental characteristics of oscillations which are damped under the action of dry friction, next we assume that viscous friction is absent ($\gamma = 0$).

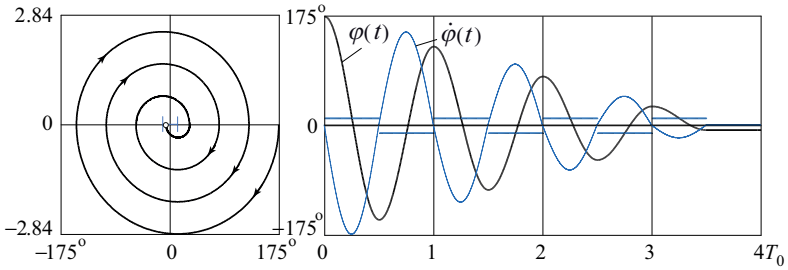

Figure 2: Damping of oscillations caused by dry friction

At the initial instant $t = 0$, let the flywheel be displaced to the right (clockwise) from the equilibrium position so that $\varphi(0) > 0$, and then released without a push. In the phase plane shown in the left-hand part of figure 2 this initial state is represented by the point which lies to the extreme right on the horizontal axis, the φ-axis. If this displacement exceeds the boundary of the stagnation interval, i.e., if $\varphi(0) > d$, the flywheel begins moving to the left ($\dot{\varphi} < 0$) and its motion is described by equation $\ddot{\varphi} + \omega_0^2(\varphi - d) = 0$. The solution to this equation with the given initial conditions ($\varphi(0) = \varphi_0$, $\dot{\varphi}(0) = 0$) is simple harmonic motion whose frequency

is ω_0. The midpoint of the motion is d. This point coincides with the right-hand boundary of the stagnation interval. The displacement d of the midpoint from zero is caused by the constant torque of kinetic friction. This torque is directed to the right (clockwise) while the flywheel is moving to the left. The initial segment of the $\varphi(t)$ graph in the right-hand part of figure 2 is the first half-cycle of the cosine curve, whose midpoint is at a height of d above the abscissa axis. The amplitude of this oscillation about the midpoint d is $\varphi_0 - d$. The corresponding portion of the phase trajectory lies below the horizontal axis. This curve is the lower half of an ellipse whose center is at the point d on the horizontal axis. This point corresponds to the right-hand boundary of the stagnation interval.

Since the amplitude of the first half-cycle is $\varphi_0 - b$, the extreme left position of the flywheel at the end of the half-cycle is $-(\varphi_0 - 2b)$. When the flywheel reaches this position, its velocity is momentarily zero, and it starts to move to the right. Since its angular velocity $\dot{\varphi}$ is subsequently positive, we must now consider equation $\ddot{\varphi} + \omega_0^2(\varphi + d) = 0$. The values of φ and $\dot{\varphi}$ at the end of the preceding half-cycle are taken as the initial conditions for this half-cycle. Thus the subsequent motion is again a half-cycle of harmonic oscillation with the same frequency ω_0 as before but with the midpoint $-d$ displaced to the left, i.e., with the midpoint at the left-hand boundary of the stagnation interval. This displacement is caused by the constant torque of kinetic friction, whose direction was reversed when the direction of motion was reversed. The amplitude of the corresponding segment of the sine curve is $\varphi_0 - 3d$. In the phase plane this stage of the motion is represented by half an ellipse lying above the φ-axis. The center of this second semi-ellipse is at the point $-d$ on the φ-axis.

Continuing this analysis half-cycle by half-cycle, we see that the flywheel executes harmonic oscillations about the midpoints alternately located at d and $-d$. The frequency of each cycle is the natural frequency ω_0, and so the duration of each full cycle equals the period $T_0 = 2\pi/\omega_0$ of free oscillations in the absence of friction. The complete phase trajectory is formed by such increasingly smaller semi-ellipses, alternately centered at d and $-d$. The diameters of these consecutive semi-ellipses lie along the φ-axis and decrease each half-cycle by $2d$. The loops of the phase curve are equidistant. The phase trajectory terminates on the φ-axis at the point at which the curve meets the φ-axis inside the dead zone (between $-d$ and d).

The joining together of these sinusoidal segments, whose midpoints alternate between the boundaries of the stagnation interval, produces the curve that describes oscillatory motion damped by dry friction (figure 2). The maximal deflection decreases after each full-cycle of these oscillations by a constant value equal to the doubled width of the stagnation interval (i.e., by the value $4d$). The oscillation continues until the end point of some next in turn segment of the sine curve occurs within the dead zone $(-d,\ d)$.

Thus, in the case of dry friction, consecutive maximal deflections diminish linearly in a decreasing arithmetic progression, and the motion stops after a final number of cycles, in contrast to the case of viscous friction, for which the maximal displacements decrease exponentially in a geometric progression, and for which the motion continues indefinitely.

Energy transformations in free oscillations damped by dry friction are shown in figure 3. While the flywheel is rotating in one direction, the torque $N_{\max}$ of kinetic friction is constant, and the total energy $E_{\text{tot}}(\varphi)$ of the oscillator decreases linearly with the angular displacement, φ, of the flywheel. This linear dependence of the total energy on φ is clearly indicated in the left-hand part of figure 3, where the parabolic potential well of the elastic spring is shown. A representing point whose ordinate gives the total energy $E_{\text{tot}}(\varphi)$ and whose abscissa gives the angular displacement of the flywheel, oscillates with time between the slopes of this well, gradually descending to the bottom of the well. The trajectory of this point consists of rectilinear segments joining the slopes of the well. These segments are straight because the negative work done by the force of dry friction is proportional to the angle of rotation, $\Delta\varphi$. The amount of

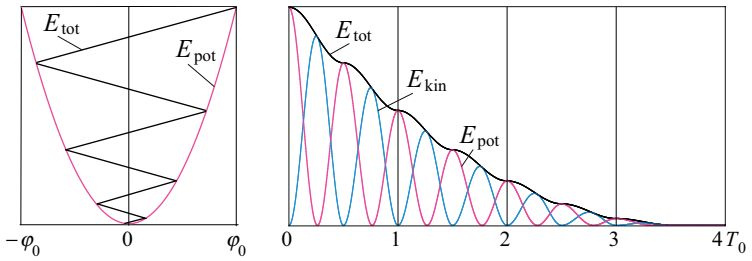

Figure 3: Energy transformations in free oscillations damped by dry friction

this work $|N_{\max}\Delta\varphi|$ equals the decrease $-\Delta E_{\text{tot}}$ of total energy.

The time rate of dissipation of the total energy, $-dE_{\text{tot}}/dt$, is proportional to the magnitude of the angular velocity, $|\dot{\varphi}(t)|$. Thus, the greatest rate of dissipation of mechanical energy through friction occurs when the magnitude of the angular velocity, $\dot{\varphi}$, is greatest, that is, when the flywheel crosses the boundaries of the dead zone. Near the points of extreme deflection, where the angular velocity is near zero, the time rate of dissipation of mechanical energy is smallest (right-hand part of figure 3).

Unlike the case of viscous friction, the oscillator with dry friction may retain some mechanical energy E_{fin} at the termination of the motion. Such occurs if the final angular displacement (within the dead zone) is not at the midpoint of the stagnation interval. Then the spring remains strained, and its elastic potential energy is not zero. The remaining energy does not exceed the value $Dd^2/2 = N_{\max}d/2$.

When the initial excitation is large enough, that is, when the initial energy is much greater than $Dd^2/2$, the oscillator executes a large number of cycles before the oscillations cease. In this case it is reasonable to consider the total energy averaged over a period of the oscillation, $\langle E_{\text{tot}}(t)\rangle$. The decrease of $\langle E_{\text{tot}}(t)\rangle$ during a large number of cycles depends quadratically on the lapse of time because the amplitude of oscillation decreases linearly with time and because the averaged total energy is proportional to the square of the amplitude. If t_{fin} is the final moment when oscillations cease, then at the time t the averaged total energy $\langle E_{\text{tot}}(t)\rangle$ is proportional to $(t - t_{\text{fin}})^2$. This statement (which clearly applies only for $t < t_{\text{fin}}$) is exactly true only when the flywheel comes to rest at the center of the stagnation interval. However, even if such is not the case and there is a residual potential energy stored in the spring after the motion ceases, the statement is approximately true.

In systems with both dry and viscous friction the damping of oscillations can also be investigated by the stage-by-stage solving of the equations of motion and by using the mechanical state at the end of the previous half-cycle as the initial conditions for the next in turn half-cycle. The phase trajectory consists in this case of the shrinking alternating halves of spiral loops that are characteristic of a linear damped oscillator. The focal points of these spirals alternate between the boundaries of the stagnation interval. The loops of the phase trajectory are no longer equidistant. Nevertheless their shrinking does not last indefinitely: the phase trajectory in this case also terminates after some finite number of turns around the origin when it reaches the stagnation interval on the φ-axis.

To figure out the relative importance of viscous versus dry friction, we can compare the decrease in amplitude caused by each of these effects during one complete cycle. It was established above that under the action of dry friction this decrease equals the constant value of the doubled width of the stagnation interval $4d$. On the other hand, viscous friction decreases the amplitude of the oscillation during a complete cycle by an amount which is proportional to the amplitude. Indeed, for $\gamma T_0 \ll 1$, i.e., for rather large values of the quality factor $Q = 2\omega_0/\gamma$,

expression for the decrease Δa during one period T_0 in the momentary amplitude a due to viscous friction can be written approximately as follows:

$$\Delta a = a(1 - e^{-\gamma T_0}) \approx a\gamma T_0 = a\gamma \frac{2\pi}{\omega_0} = \frac{\pi a}{Q}. \tag{6}$$

Equating Δa to the doubled width $4d$ of the stagnation interval, we find the amplitude $\tilde{a}$ which delimits the predominance of one type of friction over the other:

$$\tilde{a} = \frac{4d}{\gamma T_0} = \frac{4}{\pi} Qd \approx Qd. \tag{7}$$

If the actual amplitude is greater than $\tilde{a}$, the effect of viscous friction dominates. Conversely, if the actual amplitude is less than $\tilde{a}$, the effect of dry friction dominates.

When the initial excitation of the oscillator is great enough, the amplitude may exceed the value $\tilde{a} \approx Qd$. In this instance, the initial damping of the oscillations is influenced mainly by viscous friction, and the decrement in the width of several initial loops of the phase trajectory (caused by viscous friction) is greater than the separation of the centers of adjoining half-loops (i.e., the decrement exceeds the width of the stagnation interval). It is clear that in this case the shrinking of the spiral caused by viscous friction is more influential in showing the effects of damping than is the alternation of the centers of half-loops caused by dry friction.

When the value of a falls below that of $\tilde{a}$ (when $a < \tilde{a} = Qd$), the effects of dry friction dominate. In the phase plane this dominance produces a trajectory of consecutive half-loops whose centers alternately jump between the ends of the stagnation interval, $-d$ and d, until the phase trajectory reaches the segment of the φ-axis in the stagnation interval.

If viscous friction is strong, that is, if $\gamma > \omega_0$, and if the initial displacement of the flywheel $\varphi(0)$ lies beyond the boundaries of the stagnation interval, $|\varphi(0)| > d$, the released flywheel moves without oscillating toward the nearest boundary of the stagnation interval. At this point the flywheel stops turning.

5. Resonance in the oscillator with dry friction under sinusoidal excitation

In this section we analyze forced oscillations of the torsion spring pendulum in conditions of resonance, that is, when the frequency of excitation ω equals natural frequency ω_0 of the oscillator ($T = T_0 = 2\pi/\omega_0$). Generally at large enough dry friction sticking may occur: the flywheel remains at rest for a finite time after the velocity reaches zero. However, if the amplitude of excitation θ_0 in equations (4)–(5) exceeds some threshold value, the motion of the flywheel is purely sliding (non-sticking), and in the absence of viscous friction the amplitude of oscillations grows indefinitely. An example of such resonant oscillations is shown in figure 4. The phase trajectory and the graphs of $\varphi(t)$ and $\dot{\varphi}(t)$ are obtained by computer simulation which is based on numeric integration of equations (4)–(5). We note the linear growth of the amplitude: the succession of maximal deflections of the flywheel forms an arithmetic progression. Next we find analytically the threshold for excitation of such growing oscillations, and calculate the increment of the amplitude after each driving cycle.

We choose for simplicity the initial deflection $\varphi(0)$ of the flywheel coinciding with the left boundary of the dead zone, that is, $\varphi(0) = -d$, and initial angular velocity zero: $\dot{\varphi}(0) = 0$. Such initial conditions provide the sliding (non-sticking) motion from the very beginning with two turnarounds during each cycle of excitation. During the first half of the excitation period ($0 < t < T_0/2$) the angular velocity is positive ($\dot{\varphi}(t) > 0$), and we should use equation (4). The

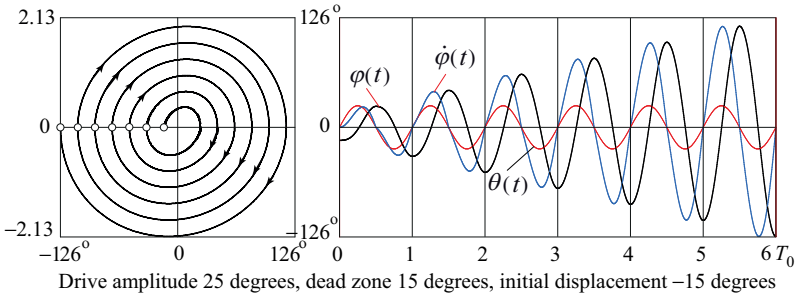

Figure 4: Oscillations at resonance with dry friction

solution to this equation (with $\gamma = 0$), satisfying the above indicated initial conditions, can be written as follows:

$$\varphi(t) = -\frac{1}{2}\theta_0(\omega_0 t\cos\omega_0 t - \sin\omega_0 t) - d, \quad \dot\varphi(t) = \frac{1}{2}\theta_0\omega_0^2 t\sin\omega_0 t, \quad 0 < t < T_0/2. \tag{8}$$

According to (8), next maximal elongation to the right side occurs at $t = T_0/2$ and equals $\frac{1}{2}\pi\theta_0 - d$. This elongation is greater in magnitude than the preceding (initial) elongation d to the left side by $\frac{1}{2}\pi\theta_0 - 2d$.

To find the increment in the amplitude during the second half-cycle of excitation, when the flywheel rotates in the opposite direction, we should use equation (5). An analytical solution to this equation is given in the Appendix. It occurs that the increment in amplitude during the second half-cycle is the same as during the first half-cycle. Therefore during the whole cycle the increment in amplitude equals $\pi\theta_0 - 4d$. Specifically, for $\theta_0 = 25°$ and $d = 15°$ (the values corresponding to the simulation shown in figure 4) the amplitude should increase during each cycle by $18.54°$. The simulation in figure 4 shows that during the first six cycles the amplitude increased by $126° - 15° = 111°$, which gives for increment during one cycle the value $18.5°$ in a good agreement with the theoretical prediction.

The growth of oscillations amplitude occurs if the value of increment $\pi\theta_0 - 4d$ during a cycle of excitation is positive. Hence the *threshold* of resonance for the oscillator with dry friction is given by the following condition:

$$\theta_0 > \frac{4}{\pi}\,d, \qquad (\theta_0)_{\min} = \frac{4}{\pi}\,d. \tag{9}$$

If the amplitude of the exciter θ_0 is smaller than the critical value $(\theta_0)_{\min}$ given by equation (9), or the dead zone d is greater than $d_{\max} = (\pi/4)\theta_0$, the flywheel, depending on the initial conditions, either remains immovable from the very beginning, or makes several movements with sticking and then finally stops at some point of the dead zone. For given width d of the dead zone (for given dry friction) equation (9) defines the critical (minimal) value $(\theta_0)_{\min}$ of the drive amplitude which provides non-sticking forced oscillations of the flywheel after a rather short transient. During the transient, depending on the initial conditions, sticking is possible. After the transient is over, at the initial moment $t_n = nT = nT_0$ of each in turn cycle of excitation, angular velocity $\dot\varphi(t_n)$ of the flywheel is zero: $\dot\varphi(nT) = 0$. This means that Poincaré sections in the phase plane (corresponding to time moments $t_n = nT$) approach the abscissa axis during the transient and remain on its negative side further on. Since the increment in the elongation is the same for each cycle, the points of Poincaré sections on the axis are equidistant (see figure 4).

Stationary periodic oscillations at the threshold conditions are shown in figure 5. At arbitrary initial values of φ and $\dot\varphi$ the phase trajectory approaches eventually the limit cycle shown in

the left-hand side of figure 5. The amplitude of steady-state forced oscillations at the threshold depends on initial conditions. If initial velocity is zero ($\dot{\varphi}(0) = 0$), steady-state oscillations occur from the very beginning, without any transient, in case initial displacement $\varphi(0)$ is negative and lies beyond the dead zone, that is, if $\varphi(0) < 0$, $|\varphi(0)| > d$. The amplitude of oscillations equals $|\varphi(0)|$. This mode of oscillations is unstable with respect to variations in parameters θ_0

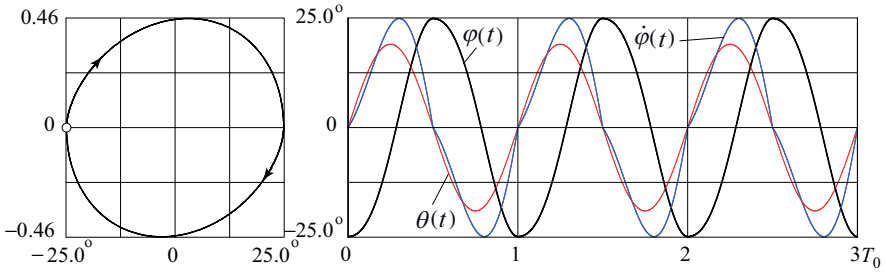

Drive amplitude 19.1 degrees, dead zone 15 degrees, initial displacement –25 degrees

Figure 5: Oscillations at the threshold conditions at resonance with dry friction

and d: a slight increment of the drive amplitude or decrement in the dead zone width causes an indefinite growth of the amplitude.

The resonant growth of amplitude over the threshold is restricted if some amount of viscous friction is present in the system. In a dual-damped system steady-state oscillations with a constant amplitude eventually establish for arbitrary initial conditions. An example of resonant oscillations in the system with both dry and viscous friction is shown in figure 6. Equations (4)–(5) allow us to calculate the amplitude a of such resonant symmetric steady-state oscillations. We choose the time origin $t = 0$ at the beginning of the next in turn drive cycle. At this moment

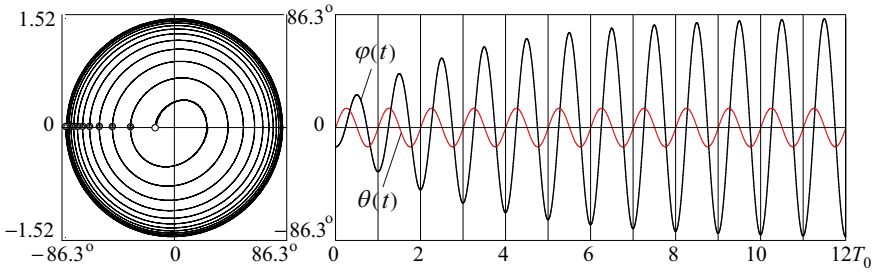

Drive amplitude 15 degrees, dead zone 5 degrees, quality 10, initial deflection –15 degrees

Figure 6: Oscillations at resonance with dry and viscous friction

the flywheel occurs at the extreme displacement to the left side ($\varphi(0) = -a$) and has the angular velocity zero ($\dot{\varphi}(0) = 0$). During the first half-cycle of the drive ($0 < t < T_0/2$) it moves to the right, so that $\dot{\varphi}$ is positive during this interval. Therefore we should use equation (4) with $\omega = \omega_0$ in its right-hand part. It is convenient to introduce instead of $\varphi(t)$ a new unknown function $\psi(t) = \varphi(t) + d$, which, according to (4), satisfies the following equation:

$$\ddot{\psi} + 2\gamma\dot{\psi} + \omega_0^2\psi = \omega_0^2\theta_0 \sin\omega_0 t. \tag{10}$$

We can search for its periodic partial solution in the form $\psi(t) = A\cos\omega_0 t$. This function satisfies equation (10), if $A = -(\omega_0/2\gamma)\theta_0 = -Q\theta_0$. Next we add to this partial solution the general solution of the corresponding homogeneous equation:

$$\psi(t) = -Q\theta_0 \cos\omega_0 t + (C\cos\omega_0 t + S\sin\omega_0 t)\exp(-\gamma t). \tag{11}$$

It follows from the initial condition $\dot{\psi}(0) = 0$ that in (11) $S = (\gamma/\omega_0)C$. To find C, we require that in the steady-state symmetric regime elongations to both sides should be equal: $\varphi(0) = -\varphi(T_0/2)$. From this condition we get

$$C = \frac{2d}{1 - \exp(-\gamma T_0/2)} = \frac{2d}{1 - \exp(-\pi/2Q)}. \tag{12}$$

Substituting these C and S values in equation (11), we obtain the time dependence of the angular displacement $\varphi(t) = \psi(t) - d$ for the first half-cycle of excitation. The desired amplitude a of this steady-state resonant oscillation is given by $-\varphi(0)$:

$$a = Q\theta_0 - d\left(\frac{2}{1 - \exp(-\pi/2Q)} - 1\right) \approx Q\left(\theta_0 - \frac{4d}{\pi}\right). \tag{13}$$

The latter approximate expression is valid in case of rather weak viscous friction, when $Q \gg 1$. In the absence of dry friction (at $d = 0$) the growth of amplitude at resonance is restricted due to viscous friction by the value $Q\theta_0$, which is Q times greater than the amplitude of the driving rod θ_0, in accordance with the first term in equation (13). With dry friction, the steady-state amplitude is approximately Q times greater than the excess of the drive amplitude θ_0 over the threshold $4d/\pi$. We emphasize that dry friction alone is unable to restrict the growth of amplitude over the threshold at $\omega = \omega_0$. Nevertheless, equation (13) shows that when dry friction is added to the system with viscous friction, the steady-state amplitude at resonance is smaller than $Q\theta_0$. From the numerical simulation (figure 6) we see that with $\theta_0 = 15^\circ$ and $Q = 10$ the resonant amplitude equals only 86.3°, if the dead zone d equals 5° (compare with $Q\theta_0 = 150^\circ$ at $d = 0$). This experimental value 86.3° is in a good agreement with the theoretical result expressed by (13), according to which the steady-state amplitude should be 86.2°.

In conditions of exact tuning to resonance (at $\omega = \omega_0$) the energy is transferred to the oscillator from the external source (from the exciter) with maximal efficiency, if at the beginning of each excitation cycle the flywheel occurs at an extreme elongation to the left-hand side. Indeed, in this case the sinusoidally varying external torque exerted on the flywheel by the exciter acts during the whole cycle in the direction of the flywheel rotation, and over the threshold (at $\pi\theta_0 > 4d$) overcomes the torque of dry friction: the amplitude grows linearly (see figure 4) increasing during a cycle by $\pi\theta_0 - 4d$. On the contrary, if at the beginning of the excitation cycle the flywheel occurs at an extreme elongation to the right-hand side, the external torque of the spring during the whole cycle is directed against the flywheel's angular velocity together with the frictional torque. In this case the amplitude reduces during each cycle by the amount $\pi\theta_0 + 4d$. After the amplitude reduces to zero, the phase relations between the flywheel and exciter change to the opposite and become favorable for the transfer of energy to the oscillator: the amplitude begins to grow.

An example of such behavior is shown in figure 7. At the drive amplitude $\theta_0 = 6.366^\circ$ and the dead zone 2.5°, the amplitude linearly reduces during each cycle of the initial stage of the process by $\pi\theta_0 + 4d = 30^\circ$. After 3 full driving cycles the amplitude diminishes from initial 90° to zero. During the further resonant growth the amplitude linearly increases during each cycle by $\pi\theta_0 - 4d = 10^\circ$, and after next 9 cycles becomes 90°.

6. Non-resonant forced oscillations

In the case of exact tuning to resonance, in contrast to the oscillator with viscous damping, dry friction alone is unable to restrict the growth of the amplitude of forced oscillations over the threshold. In non-resonant cases ($\omega \neq \omega_0$) of harmonic excitation, after a transient of a finite

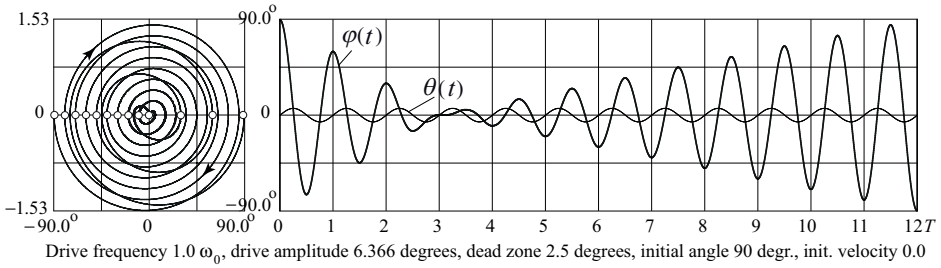

Figure 7: Phase diagram with Poincaré sections and graph of $\varphi(t)$ of oscillations with dry friction at resonance with initial deflection $\varphi(0) = +90°$.

duration, steady-state oscillations of constant amplitude can establish due to dry friction even in the absence of viscous friction. Non-resonant forced oscillations in the oscillator with dry friction received significant attention in the literature. Since the pioneer's work of Den Hartog [6] in 1930, several researchers [7]–[11] investigated the system analytically and numerically, and obtained exact solutions, describing the steady-state non-sticking motion with two turnarounds of per cycle for a harmonically excited dry friction oscillator.

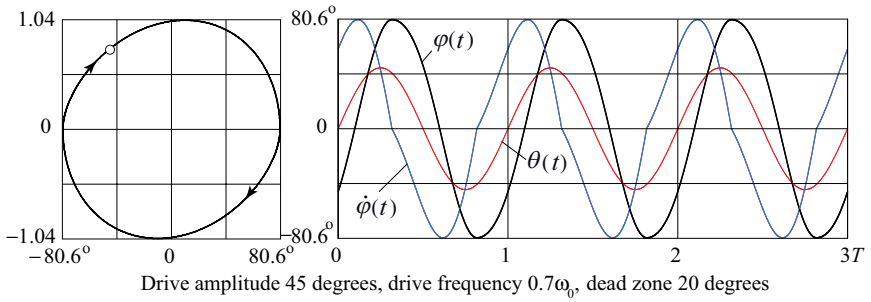

Figure 8: Phase diagram and graphs of $\varphi(t)$ and $\dot{\varphi}(t)$ of non-sticking steady-state oscillations with dry friction at $\omega = 0.7\omega_0$.

An example of such non-resonant oscillations in the system with considerable amount of dry friction is shown in figure 8. The periodic motion consists of two non-sticking phases of equal duration $T/2$. The angular velocity is negative in one phase and positive in the other. Unfortunately, we cannot express $\varphi(t)$ in a closed analytical form, because the turnaround points dividing the two phases are determined by a transcendental equation. To find the amplitude $a(\omega)$ of this symmetric oscillation, it is sufficient to consider only one phase between successive turnarounds, which is described by differential equation (5). The calculations are similar to those above described for the resonant case (though more complicated). Using periodicity and symmetrical character of the desired solution, we find the following dependence of the steady-state amplitude on the driving frequency ω:

$$a(\omega) = \theta_0 \sqrt{\frac{1}{(1-\omega^2/\omega_0^2)} - \frac{d^2(\omega_0/\omega)^2 \sin^2 \pi(\omega_0/\omega)}{\theta_0^2(\cos \pi(\omega_0/\omega)+1)^2}}. \tag{14}$$

For the frequency of excitation $\omega = 0.7\omega_0$, drive amplitude $\theta_0 = 45°$, and dead zone $d = 20°$ we get from (14) for the steady-state amplitude the value $80.63°$, which is in perfect agreement with the numerical simulation illustrated by figure 8.

Expression (14) for the steady-state amplitude of non-sticking oscillations coincides (in somewhat different notations) with results published earlier in the literature [7], [11]. Frequency-

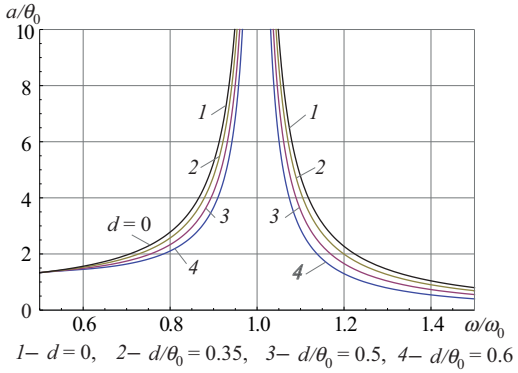

Figure 9: Amplitude–frequency characteristics of sinusoidally driven spring oscillator with dry friction damping.

response resonant curves (amplitude-frequency characteristics) given by (14) for the oscillator with dry friction are shown in figure 9 for several values of relative width d/θ_0 of the dead zone (in the frequency region $\omega > 0.5\omega_0$). We emphasize that expression (14) is valid only for sliding (non-sticking) symmetric motions of the oscillator. Such motions are possible if the following simple implicit condition (see [7]) on the parameters is fulfilled:

$$a(\omega, \theta_0, d) \geq \frac{d}{\theta_0} \left(\frac{\omega_0}{\omega}\right)^2. \tag{15}$$

Solving equation (15) numerically for the unknown d at $\omega = 0.7\omega_0$ and $\theta_0 = 45^\circ$ (these values were used for the simulation shown in figure 8), we find that the maximal width $d_{\max}$ of the dead zone for which steady-state non-sticking symmetric motions are possible equals 32.5°. A closed-form formula for the domain of steady-state symmetric non-sticking oscillatory responses was obtained in [8]. It provides the minimum driving torque amplitude $(\theta_0)_{\min}$ required to prevent sticking for given width d of the dead zone and given drive frequency ω:

$$(\theta_0)_{\min} = d\sqrt{\left(\frac{\omega_0^2}{\omega^2} - 1\right)^2 \left[1 + \frac{(\omega/\omega_0)^2 \sin^2(\pi\omega_0/\omega)}{(1 + \cos(\pi\omega_0/\omega)^2}\right]}. \tag{16}$$

Certainly, this equation can be used also to find the maximal width $d_{\max}$ of the dead zone for which steady-state non-sticking symmetric motions are possible at given frequency ω and amplitude θ_0 of the driving torque. Substituting $\omega = 0.7\omega_0$ and $\theta_0 = 45^\circ$ in (16), we get $d_{\max} = 32.5^\circ$, in accordance with the above estimate (15). The upper part of figure 10 illustrates oscillations occurring on this edge of such non-sticking regime (dead zone 32.5°). For initial conditions $\varphi(0) = 0$, $\dot{\varphi}(0) = 0$, sticking occurs several times during a short transient which ends with a non-sticking symmetric steady-state oscillations. According to (14), their amplitude must equal 66.3°, in good agreement with the simulation. For comparison, the lower part of figure 10 shows the steady-state oscillations at the same values of the frequency and amplitude of the exciter ($\omega = 0.7\omega_0$ and $\theta_0 = 45^\circ$), but for a somewhat greater dry friction (dead zone 37°). In this case sticking occurs twice during each cycle of excitation. Not surprisingly that the amplitude of symmetric forced oscillations with sticking observed in the simulation is smaller than equation (14) predicts (55° against 62°).

7. Harmonic excitation at sub-resonant frequencies

Generally characteristics of forced steady-state behavior of the oscillator with dry friction, as well as of the oscillator with viscous friction, are uniquely defined by the system parameters,

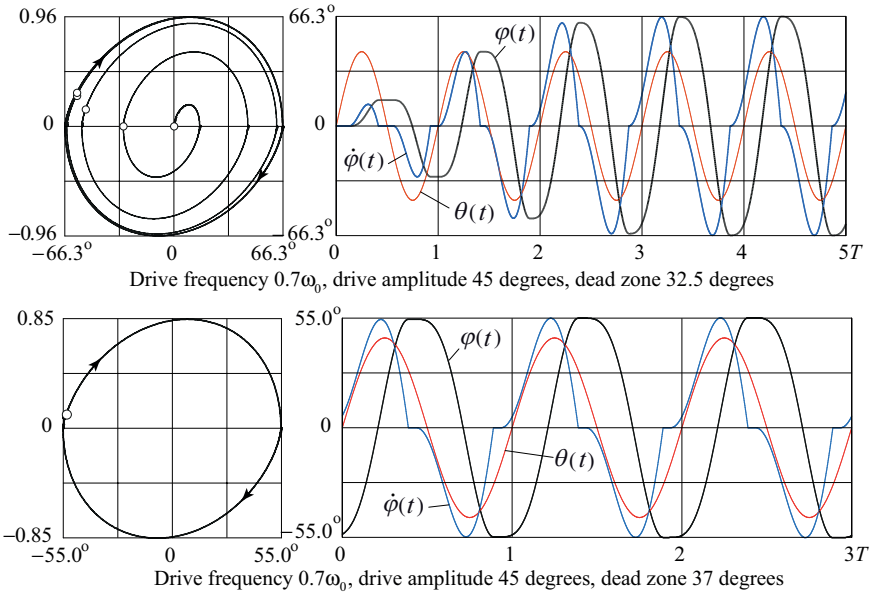

Figure 10: Phase diagram and graphs of $\varphi(t)$ and $\dot{\varphi}(t)$ of the transient that leads to non-sticking steady-state oscillations at $\omega = 0.7\omega_0$ and critical width $d = 32.5°$ of the dead zone (upper part), and steady-state symmetric oscillations with sticking at $d = 37°$ (lower part).

and by the frequency and amplitude of the excitation. Certain exceptions are revealed if the frequency ω of sinusoidal excitation coincides with one of subharmonics of the natural frequency: $\omega = \omega_0/n$, where n is an integer number. Analytical steady-state solutions at sub-harmonic excitation for the first time were considered in [12]. In the present paper we suggest a simpler and physically more transparent approach to the problem, and discuss peculiarities of such oscillations in more detail.

According to equation (14), at frequencies of excitation $\omega = \omega_0/2$, $\omega = \omega_0/4$, ...the amplitude of steady-state non-sticking symmetric oscillation, independently of the dead zone width d, should be equal to the amplitude of forced steady-state oscillation in the absence of friction (that is, at $d = 0$): $a(\omega) = \theta_0/(1 - \omega^2/\omega_0^2)$. (Certainly, this arbitrary value of d should satisfy the condition (16) for non-sticking motions, which at $\omega = \omega_0/n$ gives $d \leq \theta_0/3$.)

Figure 11 shows that frequency-response curves for different d values at $\omega = \omega_0/2$ graze the curve for $d = 0$. Computer simulations testify that in these cases steady-state oscillations are asymmetric: the angular excursion to one side is greater than to the other. This means that at $\omega = \omega_0/n$ occurrence of special solutions can be expected. Below we show that in contrast with the general case of forced oscillations, for which the steady-state regime is described by the unique solution, a continuum of asymmetric non-sticking solutions exists at $\omega = \omega_0/2n$, each of which is a limit cycle (attractor) that corresponds to initial conditions from a certain basin of attraction.

For definiteness we restrict further discussion to the case $n = 1$. If $\omega = \omega_0/2$, the spectrum of such asymmetric oscillations at sufficiently small dry friction (narrow dead zone) consists primarily of the principal harmonic with the frequency of excitation ω and its second harmonic, whose frequency 2ω equals the natural frequency ω_0 of the oscillator (see figure 12).

Mathematically, the principal harmonic corresponds to the periodic partial solution of the nonhomogeneous differential equation of motion (3) with $\gamma = 0$ and with the sinusoidal forcing

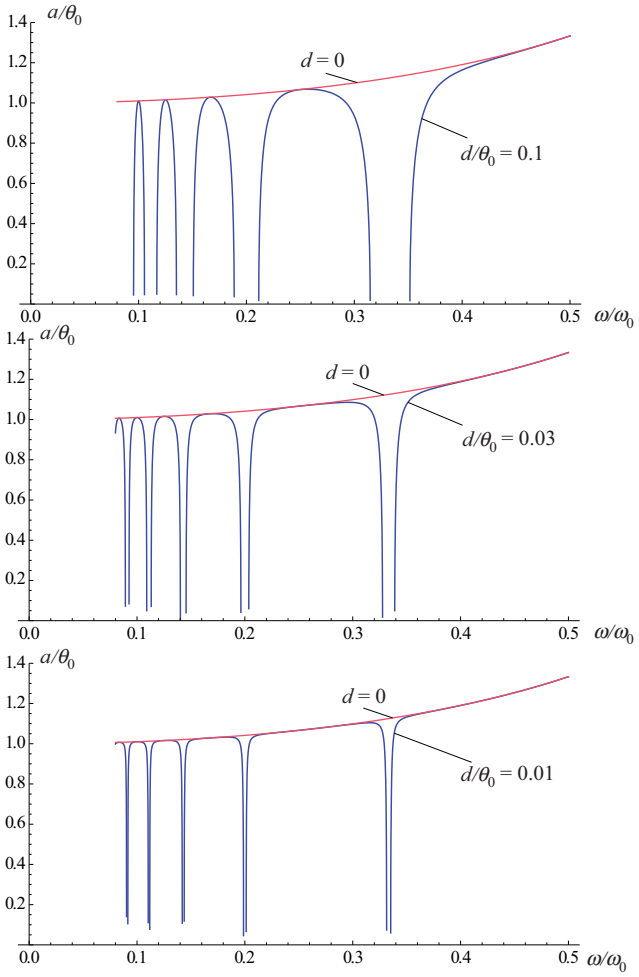

Figure 11: Frequency–response curves for the oscillator with dry friction given by equation (14) at excitation frequencies $\omega < \omega_0/2$ for several values of the dead zone width ($d/\theta_0 = 0.1$, $d/\theta_0 = 0.03$, $d/\theta_0 = 0.01$).

term $\omega_0^2\theta_0 \sin\omega t$ whose frequency ω equals $\omega_0/2$. This partial solution is $\frac{4}{3}\theta_0 \sin\omega t - d\,\mathrm{sign}\dot{\varphi}$. The second harmonic with the frequency $2\omega = \omega_0$ is the general solution of the homogeneous equation that corresponds to (3) , and can be represented (at $\gamma = 0$) as $C\cos 2\omega t + S\sin 2\omega t$, where C and S are arbitrary constants. In contrast to a system with viscous friction, now this general solution does not damp out in the course of time during the transient. The simulation shows that in the steady-state regime the phase of this second harmonic is such that $S = 0$ (see figure 12). Hence the asymmetric steady-state motion at $\omega = \omega_0/2$ can be approximately described by the following equations:

$$\varphi_+(t) = \tfrac{4}{3}\theta_0 \sin\omega t + C_+ \cos 2\omega t - d, \qquad \dot{\varphi} > 0, \tag{17}$$

$$\varphi_-(t) = \tfrac{4}{3}\theta_0 \sin\omega t + C_- \cos 2\omega t + d, \qquad \dot{\varphi} < 0, \tag{18}$$

and

$$\dot{\varphi}_+(t) = \tfrac{4}{3}\omega\theta_0 \cos\omega t - 2\omega C_+ \sin 2\omega t, \qquad \dot{\varphi} > 0, \tag{19}$$

$$\dot{\varphi}_-(t) = \tfrac{4}{3}\omega\theta_0 \cos\omega t - 2\omega C_- \sin 2\omega t, \qquad \dot{\varphi} < 0. \tag{20}$$

One condition on constants C_+ and C_- follows from the requirement of continuity of $\varphi(t)$ at the turnaround points, when the sign of velocity reverses. These are the moments $t = T/4$ and $t = 3T/4$ (see figure 12). From $\varphi_+(T/4) = \varphi_-(T/4)$ we get $C_- - C_+ = 2d$, or $C_- = C_+ + 2d$

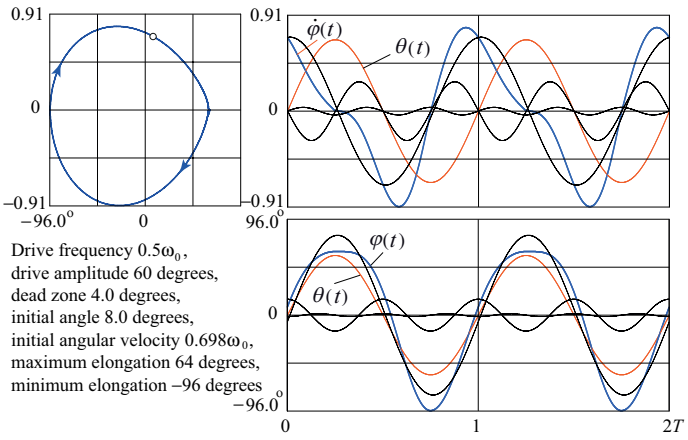

Figure 12: Phase diagram and time-dependent graphs of $\dot\varphi(t)$ and $\varphi(t)$ with the graphs of their harmonics for non-sticking asymmetric steady-state oscillations at $\omega = \omega_0/2$ and small width of the dead zone ($d = 4.0°$).

(condition $\varphi_-(3T/4) = \varphi_+(3T/4)$ yields the same relation between C_+ and C_-). Therefore only one of these constants remains arbitrary.

The steady-state regime described by equations (17)–(20) occurs from the very beginning (that is, without any transient) if the initial conditions are chosen properly. At $t = 0$ $\cos\omega t = 1$, $\sin 2\omega t = 0$, and from (19) or (20) we get that the required initial angular velocity $\dot\varphi(0) = \frac{4}{3}\omega\theta_0$. This value depends on the drive amplitude θ_0, but is independent of the dead zone width d. Since $\dot\varphi(0)$ is positive, for the required initial displacement we should use equation (17), which yields $\varphi(0) = C_+ - d$. We see that the arbitrary constants C_+ and C_-, which determine the contribution of the second harmonic into the steady-state motion, depend on the initial displacement:

$$C_+ = \varphi(0) + d, \qquad C_- = \varphi(0) + 3d. \tag{21}$$

This means that in the system with dry friction, in contrast to the oscillator with viscous friction, different initial displacements lead generally to different regimes of steady-state oscillations (to different limit cycles). Substituting these values of C_+ and C_- in (17) – (20), we get the following closed-form analytical solution for asymmetric steady-state subresonant regimes of the dry-friction oscillator at $\omega = \omega_0/2$:

$$\varphi_+(t) = \tfrac{4}{3}\theta_0 \sin\omega t + (\varphi(0) + d)\cos 2\omega t - d, \qquad \dot\varphi > 0, \tag{22}$$
$$\varphi_-(t) = \tfrac{4}{3}\theta_0 \sin\omega t + (\varphi(0) + 3d)\cos 2\omega t + d, \qquad \dot\varphi < 0, \tag{23}$$

and

$$\dot\varphi_+(t) = \tfrac{4}{3}\omega\theta_0 \cos\omega t - 2\omega(\varphi(0) + d)\sin 2\omega t, \qquad \dot\varphi > 0, \tag{24}$$
$$\dot\varphi_-(t) = \tfrac{4}{3}\omega\theta_0 \cos\omega t - 2\omega(\varphi(0) + 3d)\sin 2\omega t, \qquad \dot\varphi < 0. \tag{25}$$

Now we can derive some interesting properties of the discussed steady-state solutions. Extreme elongations correspond to the turnaround points and hence occur at $t \approx T/4$ and at $t \approx 3T/4$. Maximum displacement to the right-hand side occurs at $t \approx T/4$ and, according to equation (17) or (18), equals $\varphi_{\max} = \frac{4}{3}\theta_0 - C_+ - d$ (or, equivalently, $\varphi_{\max} = \frac{4}{3}\theta_0 - C_- + d$). Extreme elongation to the left-hand side occurs $t \approx 3T/4$ and equals $|\varphi_{\min}| = \frac{4}{3}\theta_0 + C_+ + d = \frac{4}{3}\theta_0 + C_- - d$. We see that the total angular excursion between the extreme points $\varphi_{\max} + |\varphi_{\min}|$ equals $\frac{8}{3}\theta_0$. It depends solely on the drive amplitude θ_0, and does not depend on the intensity of dry friction (on the width d of the dead zone).

The difference between the extreme elongations characterizes the asymmetry of this steady-state regime:

$$\varphi_{\max} - |\varphi_{\min}| = -2(C_+ + d) = -2(C_- - d). \tag{26}$$

The extreme elongations to both sides are equal to one another, if $C_+ = -d$ (and $C_- = d$). Such symmetric oscillation with the amplitude $\frac{4}{3}\theta_0$ occurs if the initial displacement $\varphi(0)$ equals $C_+ - d = -2d$. The phase trajectory and time-dependent graphs of $\dot\varphi(t)$ and $\varphi(t)$ (together with the graphs of their harmonics) for such symmetric oscillation are shown in figure 13. (These graphs at $d \ll \theta_0$ almost merge with the graphs of their principal harmonics.)

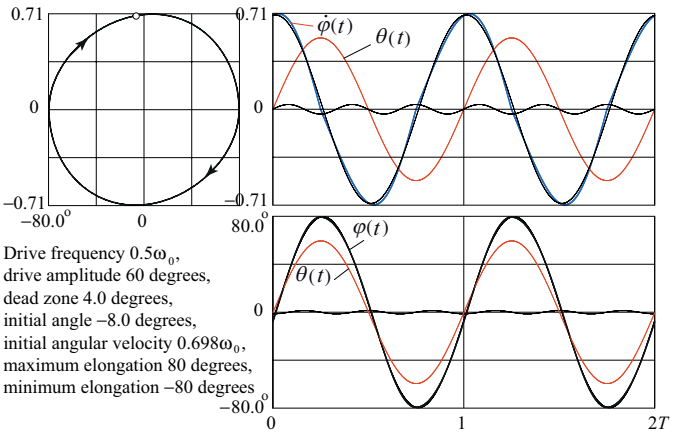

Figure 13: Phase diagram and time-dependent graphs of $\dot\varphi(t)$ and $\varphi(t)$ with the graphs of their harmonics for non-sticking symmetric steady-state oscillations at $\omega = \omega_0/2$ and small width of the dead zone ($d = 4.0°$).

Extreme elongations to one and the other side of the equilibrium position at different initial conditions, according to (21), are given by the following equations:

$$\varphi_{\max} = \tfrac{4}{3}\theta_0 - C_+ - d = \tfrac{4}{3}\theta_0 - \varphi(0) - 2d, \tag{27}$$

$$|\varphi_{\min}| = \tfrac{4}{3}\theta_0 + C_+ + d = \tfrac{4}{3}\theta_0 + \varphi(0) + 2d. \tag{28}$$

The initial conditions that lead to the greatest asymmetry of the limit cycle can be found as follows. We are interested in the unsticking regime with only two turnarounds per one excitation cycle. These turnarounds occur near $t = T/4$ and $t = 3T/4$. Therefore near each of these points the velocity graph should only once intersect the abscissa axis. This means that in the vicinity of these points $\dot\varphi(t)$ should not change sign, that is, it should satisfy the conditions $\ddot\varphi(T/4) \le 0$ (see figure 12) and $\ddot\varphi(3T/4) \ge 0$. The greatest asymmetry of oscillations corresponds to conditions $\ddot\varphi(T/4) = 0$ and $\ddot\varphi(3T/4) = 0$. The first case $\ddot\varphi(T/4) = 0$ (see figure 12), according to (20), occurs at $C_- = \frac{1}{3}\theta_0$ and hence at the initial condition $\varphi(0) = \frac{1}{3}\theta_0 - 3d$. Extreme elongations in this case, according to (27) and (28), are $\varphi_{\max} = \theta_0 + d$ and $|\varphi_{\min}| = \frac{5}{3}\theta_0 - d$.

To verify these theoretical predictions with the help of the numerical simulation (see figure 12), we choose the drive amplitude $\theta_0 = 60°$, which means that in the steady-state regime the total angular excursion between the extreme points $\varphi_{\max} + |\varphi_{\min}|$ should equal $\frac{8}{3}\theta_0 = 160°$ independently of the intensity of dry friction. In this simulation, width d of the dead zone equals $4°$, so that the steady-state oscillations with the greatest asymmetry occur from the very beginning (without any transient) at the initial conditions $\varphi(0) = \frac{1}{3}\theta_0 - 3d = 8°$, $\dot\varphi(0) = \frac{4}{3}\omega\theta_0 = \frac{2}{3}\omega_0\theta_0 = 0.698\omega_0$. The extreme elongations should be $\varphi_{\max} = \theta_0 + d = 64°$ and $\varphi_{\min} = -\frac{5}{3}\theta_0 + d = -96°$. These theoretical predictions agree perfectly well with the computer simulation (see figure 12).

Steady-state oscillations with equal elongations to both sides ($\varphi_{\max} = |\varphi_{\min}| = 80°$) at the same values of the system parameters ($\theta_0 = 60°$, $d = 4°$) occur if the initial displacement $\varphi(0) = -2d = -8°$. This case is illustrated by the simulation shown in figure 13.

The second case of the greatest asymmetry ($\dot\varphi(3T/4) = 0$) occurs, according to (19), at $C_+ = -\frac{1}{3}\theta_0$ and hence at the initial condition $\varphi(0) = -\frac{1}{3}\theta_0 - d = -24°$. Extreme elongations in this case, according to (27) and (28), are $\varphi_{\max} = \frac{5}{3}\theta_0 - d = 96°$ and $|\varphi_{\min}| = \theta_0 + d = 64°$. These asymmetric oscillations are illustrated by the simulation shown in figure 14.

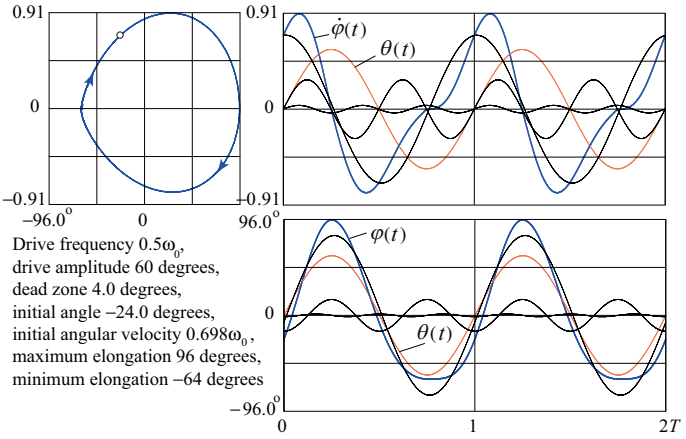

Figure 14: Phase diagram and time-dependent graphs of $\dot\varphi(t)$ and $\varphi(t)$ with their harmonics for non-sticking asymmetric steady-state oscillations at $\omega = \omega_0/2$ and small width of the dead zone ($d = 4.0°$).

Three different limit cycles of non-sticking oscillations shown in figures 12 – 14 correspond to the same values of the system parameters $\omega = \omega_0/2$, $\theta_0 = 60°$, and $d = 4.0°$. Actually, at $\omega = \omega_0/2$ there exists a continuum of different steady-state non-sticking motions with the same total angular excursion $\frac{4}{3}\theta_0$, proportional to the drive amplitude θ_0. This is a manifestation of multistability — a typical feature of nonlinear systems. If the initial angular velocity $\dot\varphi(0)$ equals $\frac{4}{3}\omega\theta_0$, and the initial angular displacement $\varphi(0)$ lies in the interval from $-\frac{1}{3}\theta_0 - d$ to $\frac{1}{3}\theta_0 - 3d$, the steady-state motion starts without a transient. The character of these steady-state oscillations vary in this interval of initial displacements from one of the most asymmetric cases at $\varphi(0) = -\frac{1}{3}\theta_0 - d$ (see figure 12) through the symmetric case occurring at $\varphi(0) = -2d$ (figure 13) to the other most asymmetric case at $\varphi(0) = \frac{1}{3}\theta_0 - 3d$ (figure 14). If the initial displacement lies beyond this interval, or the initial velocity is not equal to $\frac{4}{3}\omega\theta_0$, one of the limit cycles from the same continuum is eventually established after a transient process, during which oscillations with sticking for finite time intervals take place.

Not surprisingly that if even a small amount of viscous friction is present in the system, the above considered asymmetric regimes can be observed only at the initial stage: after a long transient oscillations become symmetric, like those shown in figure 13. Indeed, the asymmetry is caused by the contribution of the second harmonic, which corresponds to natural oscillations with the frequency $\omega_0 = 2\omega$. Mathematically, this second harmonic is the the general solution of the homogeneous differential equation. In the presence of viscous friction, these natural oscillations damp out during the transient.

Steady-state non-sticking sub-resonant forced oscillations of the above considered type exist if dry friction is not strong enough for the given drive amplitude. To find this restriction, it is sufficient to equate the expressions for the extreme elongations $\varphi_{\max} = \theta_0 + d$ and $|\varphi_{\min}| = \frac{5}{3}\theta_0 - d$ for the most asymmetric case. This yields $d_{\max} = \theta_0/3$. At $d = \theta_0/3$ there exists only one (symmetric) limit cycle with the amplitude $\varphi_{\max} = \frac{4}{3}\theta_0$. At greater values of the dead zone width ($d > \theta_0/3$) only steady-state oscillations with sticking are possible.

Similar peculiarities are characteristic of forced oscillations with dry friction, sinusoidally excited at other sub-resonant frequencies of even orders $\omega = \omega_0/(2n)$. In particular, for $\omega = \omega_0/4$ a continuum of non-sticking asymmetric steady-state motions exists for the same values of the system parameters, if the width d of the dead zone does not exceed $\frac{1}{15}\theta_0$, where θ_0 is the drive amplitude. Each of these motions occurs without a transient, if the initial velocity equals $\frac{4}{15}\omega_0\theta_0$, and the initial displacement lies in the interval between $-\frac{1}{15}\theta_0 + d$ and $\frac{1}{15}\theta_0 - d$.

At sub-resonant frequencies of odd orders $\omega = \omega_0/(2n+1)$ non-sticking solutions for an oscillator with dry friction do not exist: at least twice during each cycle of the steady-state motion velocity turns to zero for finite time intervals. Such two-stop-two-slip motions consisting of two stick phases and two slip phases in a dry friction oscillator are investigated in [17].

8. Concluding remarks

In this paper we concentrated on peculiarities in behavior of a simple mechanical system — torsion spring oscillator with dry and viscous friction. The intensity of dry friction is characterized by the width d of the dead zone. The amplitude of non-forced oscillations reduces under dry friction during each cycle by the same amount $4d$, proportional to the dead zone width, and the whole process takes a finite time. Under sinusoidal forcing, dry friction cannot restrict the growth of resonant oscillations: at $\omega = \omega_0$ the amplitude grows indefinitely, increasing in each cycle through $\pi\theta_0 - 4d$, if the drive amplitude θ_0 exceeds the threshold value $4d/\pi$.

In non-resonant cases ($\omega \neq \omega_0$) of harmonic excitation, after a transient of a finite duration, steady-state oscillations of a finite amplitude can establish due to dry friction even in the absence of viscous friction. Generally, such periodic motion consists of two symmetric non-sticking phases of equal duration $T/2$, if, for the given width d of the dead zone, the drive amplitude θ_0 is large enough to prevent sticking. The steady-state amplitude of these symmetric oscillations for given ω uniquely depends on θ_0 and d. At sub-resonant frequencies of excitation $\omega = \omega_0/n$ ($n = 2, 4, \ldots$) certain peculiarities of forced oscillations reveal themselves. In particular, a continuum of different non-sticking steady-state oscillations can exist for the same values of the system parameters θ_0 and d. This is a manifestation of multistability — a characteristic feature of nonlinear systems. Such oscillations are generally asymmetric: the angular elongation to one side is greater than to the other, though the total angular excursion between the extreme (turnaround) points is the same for given value of the drive amplitude θ_0 (and is independent of the dead zone width d). The asymmetry of a certain steady-state regime of this continuum depends on the initial conditions. Among each continuum of such solutions coexisting at given values of θ_0 and d, there is a single symmetric oscillation.

Appendix. Analytical solution for the second half-cycle of resonant excitation

For the first half-cycle of excitation at resonance ($\omega = \omega_0$) the motion of the flywheel is given by equation (8), if initially the flywheel is at rest ($\dot\varphi(0) = 0$) exactly at the left side of the stagnation zone: $\varphi(0) = -d$. If we take some arbitrary initial deflection $\varphi(0) = \varphi_0$ to the left side from the equilibrium ($\varphi_0 < 0$) which lies beyond the dead zone ($|\varphi_0| > d$) and initial velocity $\dot\varphi(0) = 0$, the motion of the flywheel will also be non-sticking from the very beginning, and during the time interval $0 < t < T_0/2$ will be described by the following expression:

$$\varphi(t) = (\varphi_0 + d)\cos\omega_0 t - \frac{1}{2}\theta_0(\omega_0 t\cos\omega_0 t - \sin\omega_0 t) - d, \quad 0 < t < T_0/2. \tag{29}$$

At the end of the first half-cycle (at $t = T_0/2$) the angular velocity of the flywheel becomes zero, while its deflection to the right side reaches $\varphi_1 = -\varphi_0 + \frac{1}{2}\theta_0\pi - 2d$. These values of φ

and $\dot{\varphi}$ should be used as the initial conditions at $t = T_0/2$ for the differential equation (5) that describes (with $\gamma = 0$) the second half-period $T_0/2 < t < T_0$ of the forced motion, during which $\dot{\varphi} < 0$. To solve this equation, it is convenient to move the time origin $t = 0$ to $T_0/2$. In these new notations equation (5) takes the following form:

$$\ddot{\varphi} + \omega_0^2(\varphi + d) = -\omega_0^2\theta_0 \sin\omega_0 t. \tag{30}$$

Solution to equation (30), satisfying initial conditions $\varphi(0) = \varphi_1$ and $\dot{\varphi}(0) = 0$, can be written as follows:

$$\varphi(t) = (\varphi_1 - d)\cos\omega_0 t + \frac{1}{2}\theta_0(\omega_0 t\cos\omega_0 t - \sin\omega_0 t) + d. \tag{31}$$

To find the angular position $\varphi(T_0)$ and the angular velocity $\dot{\varphi}(T_0)$ of the flywheel at the end of the first cycle of excitation, we should substitute $t = T_0/2$ into equation (31):

$$\varphi(T_0) = -\varphi_1 + d - \frac{1}{2}\theta_0\pi + d = \varphi_0 - \theta_0\pi + 4d. \tag{32}$$

Hence the magnitude of angular elongation to the left increased during the first cycle of excitation by the value $|\varphi(T_0) - \varphi_0| = \pi\theta_0 - 4d$. This increment is independent of the initial deflection φ_0, so that the succession of maximal deflections at resonance in the oscillator with dry friction forms an increasing arithmetic progression.

In case $d = 0$ (zero width of the dead zone, that is, absence of dry friction) the solution given by equation (29) takes the following form:

$$\varphi(t) = \varphi_0\cos\omega_0 t - \frac{1}{2}\theta_0(\omega_0 t\cos\omega_0 t - \sin\omega_0 t). \tag{33}$$

Obviously, for initial conditions $\varphi(0) = \varphi_0$, $\dot{\varphi}(0) = 0$ this solution is valid for any t value, not only for the first half-cycle of excitation $0 < t < T_0/2$. According to equation (33), in the absence of any friction (dry and viscous), the amplitude of resonant forced oscillations changes in magnitude during one cycle of excitation by the same amount $\pi\theta_0$. If the oscillator is excited from the state of rest in the equilibrium position, its amplitude grows linearly from the very beginning. This growth continues indefinitely. From the energy considerations, this can be easily explained by certain phase relations between rotary oscillations of the flywheel and the sinusoidally varying torque exerted on the flywheel by the spring: this torque acts always in the direction of rotation, increasing thus the energy of the flywheel.

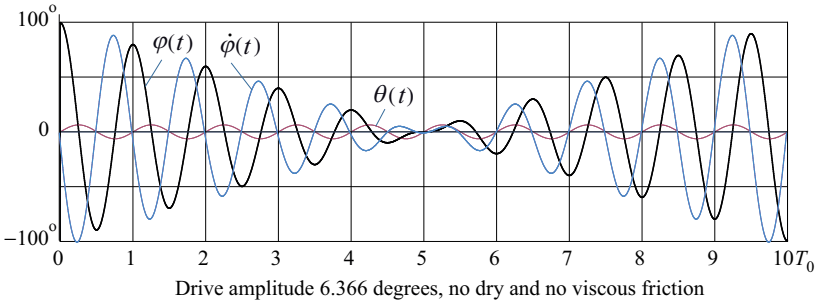

Figure 15: Oscillations at resonance without friction (with initial displacement).

However, if the initial displacement of the flywheel is positive ($\varphi(0) > 0$), the external torque at the initial stage is directed against the angular velocity, and the amplitude of oscillations diminish, in spite of the exact tuning to resonance, through value $\pi\theta_0$ during each cycle.

The energy is transferred from the oscillator to the exciter. This situation is illustrated in figure 15. After the amplitude reduces to zero, the phase relations between the exciting rod and the flywheel become favorable for the transfer of energy to the oscillator, and the amplitude starts to grow indefinitely. In the absence of dry friction, the initial linear reduction and further growth of the amplitude occur equally fast, in contrast to the case with dry friction (see figure 7), in which friction speeds up the reduction and slows down the growth of the amplitude.

[1] B. Feeny, A. Guran, N. Hinrichs, K. Popp, A historical review on dry friction and stickslip phenomena, ASME Applied Mechanics Reviews **51** 321–341, 1998.

[2] A. B. Pippard, The physics of vibration (The simple classical vibrator). Cambridge University Press, 1978.

[3] E. I. Butikov, Physics of Oscillations, Users Manual. American Institute of Physics, Physics Academic Software, New York, 1996.

[4] L. M. Burko, A Piecewise-Conserved Constant of Motion for a Dissipative System, Eur. J. Phys. **20**, 281–288, 1999.

[5] A. Marchewka, D. S. Abbott, R. J. Beichner, Oscillator damped by a constantmagnitude friction force. AJP **72**, 477–483, 2004.

[6] J. P. Den Hartog, Forced vibrations with combined Coulomb and viscous damping, Transactions of the American Society of Mechanical Engineers **53**, 107–115, 1930.

[7] S. W. Shaw, On the dynamic response of a system with dry friction, Journal of Sound and Vibration **108**, 305–325, 1986.

[8] H.-K. Hong, C.-S. Liu, Non-sticking oscillation formulae for Coulomb friction under harmonic loading, Journal of Sound and Vibration **244**, 883–898, 2001.

[9] J. W. Liang, B. F. Feeny, Identifying Coulomb and Viscous Friction in Forced Dual-Damped Oscillators, Journal of Vibration and Acoustics **126**, 118–125, 2004.

[10] A. C. J. Luo, B. C. Gegg, Stick and non-stick periodic motions in periodically forced oscillators with dry friction, Journal of Sound and Vibration **291**, 132–168, 2006.

[11] G. Csernak, G. Stepan, On the periodic response of a harmonically excited dry friction oscillator. Journal of Sound and Vibration **295**, 649–658, 2006.

[12] G. Csernak, G. Stepan, S. W. Shaw, Sub-harmonic resonant solutions of a harmonically excited dry friction oscillator, Nonlinear Dynamics, **53**, 93–109, 2007.

[13] S. Chatterjee, Resonant locking in viscous and dry friction damper kinematically driving mechanical oscillators, Journal of Sound and Vibration **332**, 3499–3516, 2013.

[14] A. C. J. Luo, Regularity and Complexity in Dynamical Systems, Springer, 2011.

[15] F. J. Elmer, Nonlinear dynamics of dry friction, J. Phys. A: Math. Gen. **30**, 6057–6063, 1997.

[16] A. F. Filippov, Differential Equations with Discontinuous Righthand Sides, Mathematics and its Applications (Soviet Series), vol. 18, Kluwer, Dordrecht, 1988.

[17] S. P. Yang, S. Q. Guo, Two-stop-two-slip motions of a dry friction oscillator, Sci. China Tech. Sci. **53**, 623–632, 2010.